JOURNAL OF CATALYSIS 103, 105–114 (1987)

Characterization and Catalytic Activity of Unsupported Nickel–Rhenium Catalysts Modified by Calcium Oxide

S. ENGELS,*,[1] J. EICK,* W. MÖRKE,* U. MAIER,* I. BÖSZÖRMÉNYI,† K. MATUSEK,† Z. SCHAY,† AND L. GUCZI†,[1]

* *Technische Hochschule "Carl Schorlemmer" Leuna-Merseburg DDR-4200, Merseburg, Germany (DDR); and † Institute of Isotopes of the Hungarian Academy of Sciences, P.O. Box 77, H-1525 Budapest, Hungary*

Received September 6, 1984; revised January 29, 1986

Unsupported nickel–rhenium bimetallic catalysts have been prepared from a mixture of NH_4ReO_4 and nickel oxide containing CaO. It has been established that the total and metal surface areas as measured by X-ray diffraction, by the BET method and by CO chemisorption are enhanced by CaO addition compared to calcium-free samples. In addition, alloy formation is promoted by CaO, as indicated by ferromagnetic resonance (FMR) and X-ray diffraction measurements. X-Ray photoelectron spectroscopy reveals surface enrichment of rhenium and calcium abundance on the surface, particularly in heat treated samples. Sintering is retarded by the presence of CaO. The turnover frequencies for the dehydrogenation of cyclohexane, for the hydrogenation of benzene, and for the hydrogenolysis of ethane increase with increasing addition of Re to Ni up to the composition of 85 at.% Re–15 at.% Ni, followed by a fall for the pure rhenium catalyst. A remarkable effect of calcium addition is a strong suppression in the specific rate of ethane hydrogenolysis. For CO hydrogenation the TOF increases as the amount of nickel decreases and there is a simultaneous change in the olefin and C_2^+ selectivity. In the range between pure Ni and 85 at.% Ni–15 at.% Re the formation of higher hydrocarbons is slightly promoted whereas on the Re-rich samples a high methane selectivity can be observed due to the enhanced hydrogenation activity of rhenium.

INTRODUCTION

Earlier it was found that the addition of rhenium to nickel results in the enhancement of nickel dispersion (*1–3*). However, nickel compounds often contain small amounts of calcium oxide as impurity, and thus it is important to find out the effect of a nonreducible metal oxide on the formation of a bimetallic catalyst.

It has been known for a long time that some nonreducible oxides serve as promoters in ammonia synthesis and steam reforming catalysts (*4, 5*). Generally speaking, the presence of such oxide species in mono- or bimetallic systems is supposed to result in the stabilization of small metal particles (*6–10*).

The main goal of this work is to clarify the effect of calcium oxide present in an amount larger than that normally observed in the nickel catalyst, for the nickel–rhenium system. The samples prepared are characterized by several physical methods and by hydrocarbon reactions as well as by the hydrogenation of carbon monoxide.

EXPERIMENTAL

Catalysts. Calcium-containing nickel oxide samples were prepared from nickel carbonate by decomposition at 770 K. The determination of calcium was carried out by the atomic absorption method. NH_4ReO_4 and nickel oxide containing calcium oxide were slurried at 330–340 K in varying compositions and dried at 350 K. The powders were reduced in hydrogen (5 liters/h) at 670 K for 6 h. The preparation has been detailed elsewhere (*2*). In some cases an additional heat treatment (these samples are denoted by HT) in hydrogen at 920 K for 6 h was applied. The calculated composition

[1] To whom correspondence should be addressed.

0021-9517/87 $3.00

TABLE 1

Nominal Composition of the Catalyst Samples in at.%

Catalysts	Ni	Ca	Re
100 Ni	99	1	—
98Ni2Re	97.02	0.98	2
95Ni5Re	94.05	0.95	5
92Ni8Re	91.08	0.92	8
90Ni10Re	89.1	0.9	10
85Ni15Re	84.15	0.85	15
80Ni20Re	79.2	0.8	20
70Ni30Re	69.3	0.7	30
50Ni50Re	49.5	0.5	50
30Ni70Re	29.7	0.3	70
15Ni85Re	14.85	0.15	85
100Re	—	—	100
Re + Ca	—	1	99

of the samples is given in Table 1. The pure rhenium catalyst was prepared by decomposition of NH_4ReO_4 in a stream of hydrogen at 670 K. The 1 at.% Ca-containing rhenium catalyst was also prepared by adding $Ca(OH)_2$ to NH_4ReO_4 before the reduction step and is denoted as Re + Ca catalyst.

Characterization of the bimetallic samples. The surface area of the catalysts was measured by low temperature nitrogen adsorption (BET method) and by CO chemisorption in a pulse system (*2*). Several physical methods were applied to determine the structure of the bimetallic samples. X-Ray diffraction served to follow the reduction and the phase composition. The ferromagnetic resonance (FMR) method (*3*) was utilized to follow alloy formation in the system. The surface composition of the rhenium–nickel samples was measured by X-ray photoelectron spectroscopy (XPS) using a Kratos ES 300 spectrometer with an Al$K\alpha$ (1486.6 eV) X-ray source.

Catalytic reactions. Hydrogenation of benzene and dehydrogenation of cyclohexane were carried out in a tubular flow reactor. Normally 200 mg catalyst diluted with 800 mg quartz sand was charged into the reactor. The passivated catalysts were reduced *in situ* at 670 K in a stream of hydrogen (5 liters/h) for 2.5 h. After reduction the cyclohexane at 2.45 ml/h flow rate was introduced into the H_2 stream and its conversion to benzene was measured at 570 K after 120 min on stream. For benzene hydrogenation the reactor temperature was adjusted to 420 K and 2.46 ml benzene/h was introduced into the H_2 stream. Hydrogenolysis of ethane was carried out in a pulse system. The flow rate of hydrogen was 3 liters/h and 1 ml ethane was pulsed in the stream. A reaction temperature between 550 and 700 K was selected to obtain a conversion in the 5–30% range. The catalytic activity was evaluated by the method introduced by Basset and Habgood (*11*) assuming first order kinetics for ethane.

The H_2 + CO reaction was measured in a flow reactor operated at differential conversion level. A 3 : 1 H_2/CO mixture was introduced in the reactor with a flow rate of 0.9 liters/h between 470 and 630 K, depending on the activity of the catalysts. The reaction products were analyzed by a gas chromatograph (Packard Type 427) using an *n*-octane on Porasil C column with a temperature program. The catalytic activity referred to as the amount of CO producing hydrocarbons was expressed by the rate in mol s^{-1} g^{-1}_{cat}. The specific activity here is calculated as turnover frequency (TOF) (s^{-1}), using the number of metallic sites determined by CO chemisorption. The $S_{C_1^+}$ and $S_{olef.}$ values used to describe selectivities are defined as $\Sigma_2 C_i/\Sigma_1 C_i$ and $\Sigma_2 C_i^=/\Sigma_2 C_i$, respectively, where C_i and $C_i^=$ are the moles of hydrocarbons and the moles of olefins with carbon number i, respectively.

RESULTS

1. X-Ray Diffraction

Earlier it was shown that at 670 K alloy formation for the calcium-free nickel–rhenium catalysts (*2*) takes place only to a small extent, in agreement with the phase diagram (*12*). For the calcium-containing catalysts alloy formation is again far from being complete because in the X-ray diffraction pattern two phases, a hexagonal

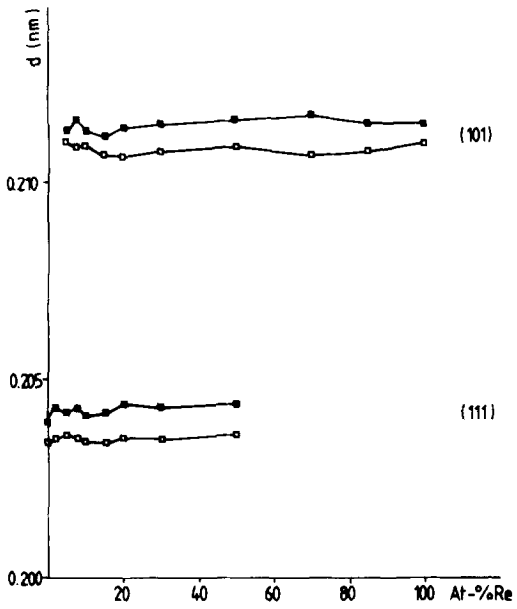

FIG. 1. Lattice distances determined from hcp (101) and fcc (111) reflections vs composition with accuracy of ±0.0005 nm. Symbols: (■) Ca-containing catalysts, (□) Ca-free samples.

closed packed (hcp) and a face-centered cubic (fcc) phase can be seen. In Fig. 1 the (101) and the (111) reflections have been evaluated for the hcp and fcc phases, respectively, to determine the lattice distance. For comparison, data for the calcium-free catalysts from Ref. (*2*) are also included. It can be seen that the addition of calcium results in an increase in the lattice distance, which could be an indication for alloy formation.

In Table 2 the apparent particle size of the catalyst samples is presented. The calculation is based on the X-ray line-broadening of the (111) and (200) reflections using the Scherrer equation (*13*). It is quite clear that the addition of calcium results in a decrease in the crystallite size. The same holds for the addition of rhenium to nickel. On heat treatment in hydrogen at 920 K there is only a slight increase in the crystallite size for the catalysts containing more than 10 at.% Re, whereas a significant sintering can be observed for the nickel-rich catalysts.

2. *Ferromagnetic Resonance (FMR) Measurements*

Phase formation in a multimetallic catalyst can be followed by the FMR technique (*3*).

Since the magnetization of a sample is directly proportional to the line intensity, I (*14*), alloy formation can be followed by the I vs composition curve (see Fig. 2). The decrease of I with increasing rhenium content can be ascribed to the increasing alloy formation which is further enhanced by heat treatment. This explanation is based upon the fact that any changes in the line intensity due to the variation in dispersion are negligible, since the X-band is saturated above sizes of 10 nm (*15*).

3. *X-Ray Photoelectron Spectroscopy (XPS)*

The surface composition of the samples and the chemical state of nickel and rhenium were studied by XPS. Prior to the measurements the passivated samples were reduced at 670 K for 4 in a hydrogen flow of

TABLE 2

Apparent Particle Size of the Crystallites in fcc Phase[a] in nm

Sample	Without CaO[b] Standard reduction (670 K)	With CaO	
		Standard reduction (670 K)	HT[c] (920 K)
100Ni0Re	58.5[d]	17.3	45.7
98Ni2Re	34.3	15.4	36.9
95Ni5Re	47.0	15.6	31.3
92Ni8Re	33.9	14.8	24.7
90Ni10Re	34.8	15.4	18.7
85Ni15Re	31.7	14.3	15.5
80Ni20Re	31.7	13.6	12.2
70Ni30Re	30.7	11.6	12.8
50Ni50Re	26.1	—	14.8
30Ni70Re	—	—	15.5

[a] Calculated from (111) and (200) reflections using the Scherrer equation.

[b] Reproduced from Ref. (*2*).

[c] Heat treated in hydrogen.

[d] Uncertainty at 60 nm $^{+30}_{-10}$ nm and at 10 nm $^{+1.3}_{-1.0}$ nm.

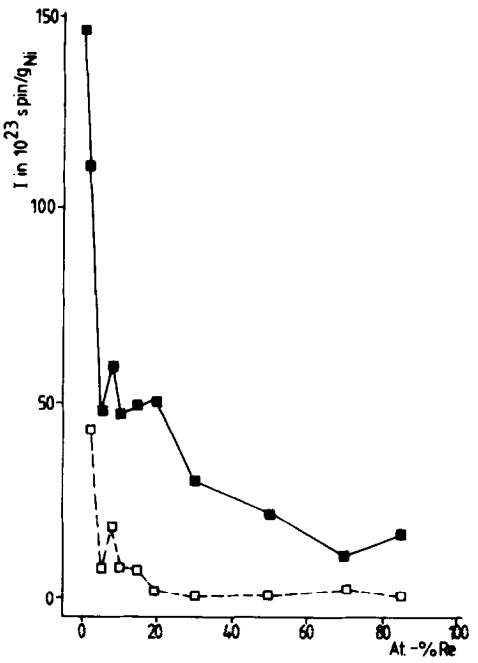

FIG. 2. Line intensity, I, measured in the FMR absorption of the Ca-containing catalysts. Symbols: (■) reduced at 670 K, (□) heat treated samples.

5 liters/h followed by an *in situ* reduction in 13 Pa hydrogen at 520 K in the sample preparation chamber. Peak positions for the Ni $2p_{3/2}$ and Re $4f_{7/2}$ transitions are given in Fig. 3. The C 1*s* peak at 284.5 eV binding energy (B.E.) from carbon contamination is taken as an internal standard for the determination of the B.E. for nickel and rhenium. The uncertainty in the B.E. values is 0.2 eV. The addition of calcium to nickel results in a 0.5 eV shift of the Ni $2p_{3/2}$ peak toward higher B.E. (for metallic Ni the peak position is 852.3 eV). On addition of rhenium to the calcium-containing nickel catalysts there is a further increase of about 0.3 eV. The Re $4f_{7/2}$ peak is also shifted to higher B.E. by 0.3 eV for the Re + Ca sample and for the nickel-containing catalysts, but the shift seems to be independent of the nickel concentration within the experimental error. In Fig. 4 the Ni $2p$ and Re $4f$ regions are presented for the 50 at.% Re catalyst. The shoulder on the high B.E. side of the Ni $2p_{3/2}$ peak is caused by nickel oxide, present in a quantity of 5–10%.

The average surface composition of the

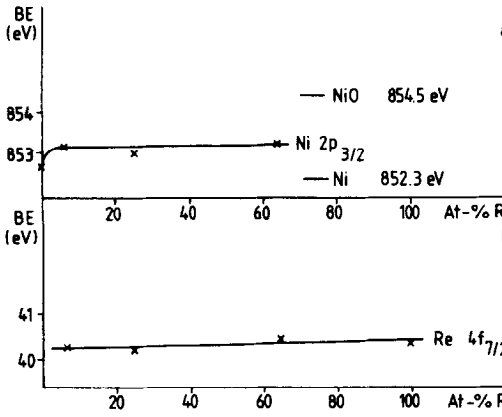

FIG. 3. Change of binding energy, B.E., for rhenium $4f_{7/2}$ and nickel $2p_{3/2}$ lines vs composition for Ca-containing samples.

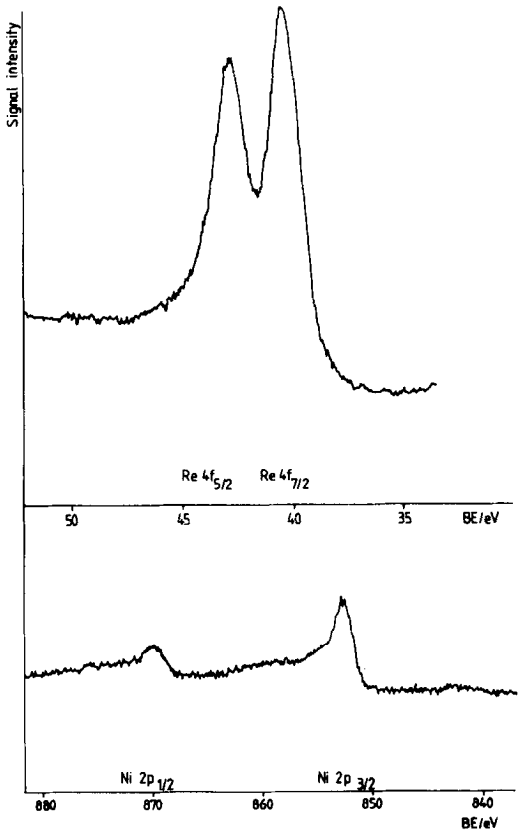

FIG. 4. XPS spectra for rhenium $4f$ and nickel $2p$ regions for the Ca-containing sample at 50 at.% Re composition.

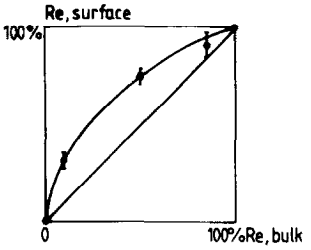

FIG. 5. Surface Re/(Ni + Re) ratio vs bulk concentration of rhenium in the Ca-containing samples.

catalysts is calculated from the peak areas using standard procedures (*16*) in which corrections are allowed for ionization cross sections, escape depths for electrons, and for spectrometer transmission. A surface enrichment in rhenium is observed for the calcium-containing catalysts, as given in Fig. 5. A pronounced surface enrichment in calcium is found for high nickel concentration resulting in nearly a monolayer of CaO in the nickel sample. On decreasing the nickel concentration the surface composition of Ca with regard to nickel decreases, but 5–20% of the surface is always covered with calcium.

The effect of heat treatment is to produce a small change in the relative concentration of Re and Ni and a large increase of the Ca concentration on the surface, as shown in Table 3.

4. *Surface Area Measurements*

In Fig. 6 the BET surface area is plotted vs the rhenium content of the samples for calcium-containing and for calcium-free samples, both having been reduced by the standard procedure. The effect of calcium resulting in the increase of dispersion (already indicated by the X-ray diffraction measurement) is obvious from the BET data. This effect is significant even at low nickel content. However, heat treatment of the samples drastically decreases the BET surface area.

TABLE 3

Surface Concentration of Ni, Re, and Ca on the 50Ni50Re Catalyst

Element	Atom%	
	H_2/670 K	H_2/920 K
Re	69	64
Ni	20	19
Ca	11	17

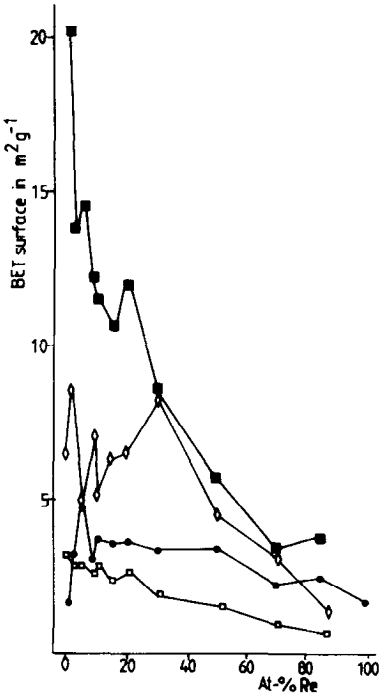

FIG. 6. BET surface area vs composition for the nickel–rhenium samples. Symbols: (■) Ca-containing samples reduced at 670 K, (●) Ca-free samples reduced at 670 K from Ref. (*17*), (□) Ca-containing samples heat treated at 920 K for 6 h, (◇) surface area calculated from CO chemisorption for the Ca-containing samples.

The effect of calcium on the metal surface area measured by CO chemisorption is presented in Fig. 7. Here again the presence of calcium enhances the CO chemisorption indicating higher metal dispersion. The increase is about 10-fold for the Ca + Re catalyst, whereas only two- to three-fold for the nickel-containing samples.

From CO chemisorption the specific metal surface area can also be calculated assuming a 1 : 1 stoichiometry for the CO

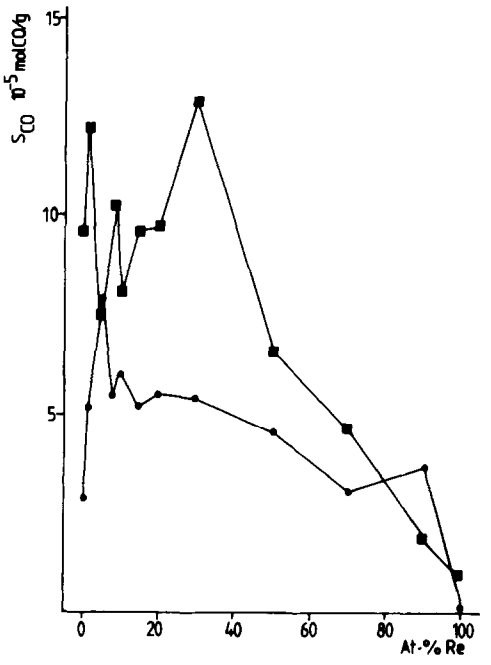

FIG. 7. CO chemisorption vs composition for the samples reduced at 670 K. Symbols are as in Fig. 6.

chemisorption and an average surface density of 10^{19} atoms m^{-2}. The values obtained are below the BET surface area as indicated in Fig. 6. Since the total and metal surface areas are the same for the calcium-free bimetallic catalysts (*2*), the conclusion can be drawn that calcium partly covers the metal sites, which is in agreement with the XPS data. Nevertheless, the metal surface area is still higher here than in the calcium-free samples.

5. *Catalytic Reactions*

Dehydrogenation of cyclohexane, hydrogenation of benzene, hydrogenolysis of ethane, and hydrogenation of carbon monoxide have been studied to test the catalytic activity. First we present in Fig. 8a the TOF values vs composition for calcium-free catalysts calculated from the data published in Ref. (*17*). Cyclohexane dehydrogenation is completely independent of the change of dispersion induced by rhenium. For benzene hydrogenation and ethane hydrogenolysis the increased metal dispersion up to 8 at.% Re is accompanied by a sharp increase of the TOF. However, for benzene hydrogenation the TOF runs parallel with the decrease of dispersion induced by further rhenium addition. On the other hand, the TOF for ethane hydrogenolysis keeps increasing even at higher rhenium content reaching a maximum at about 50 at.% Re, similar to that found for *n*-butane hydrogenolysis measured on the Pt–Re system (*18*).

Despite the enhanced metal surface area for calcium-containing nickel, the TOF is 1.5–3 orders of magnitude smaller than that on calcium-free samples. As shown in Fig. 8b, the addition of rhenium causes a sharp increase in the TOF for all hydrocarbon reactions up to the composition of 85 at.% Re and the TOF drops again on the pure rhenium catalyst. It is of importance to note that the increase of the TOF for hydrogenation of benzene and for hydrogenolysis of

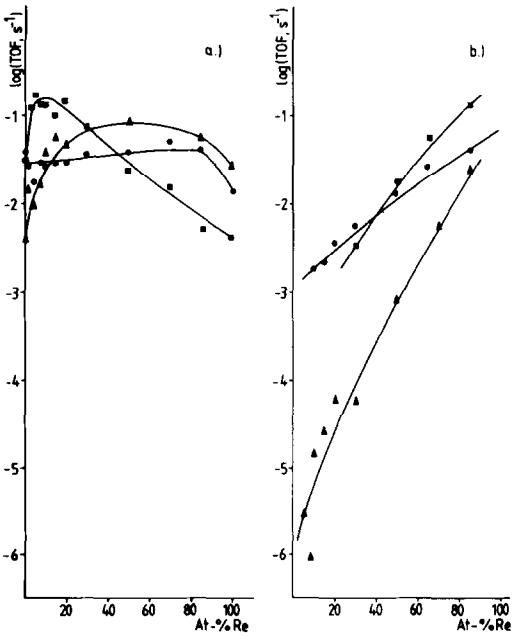

FIG. 8. Turnover frequencies (s^{-1}) vs composition on the samples reduced at 670 K. (a) Ca-free catalysts, (b) Ca-containing catalysts. Symbols: (●) dehydrogenation of cyclohexane at 570 K, (■) hydrogenation of benzene at 420 K, (▲) hydrogenolysis of ethane at 570 K.

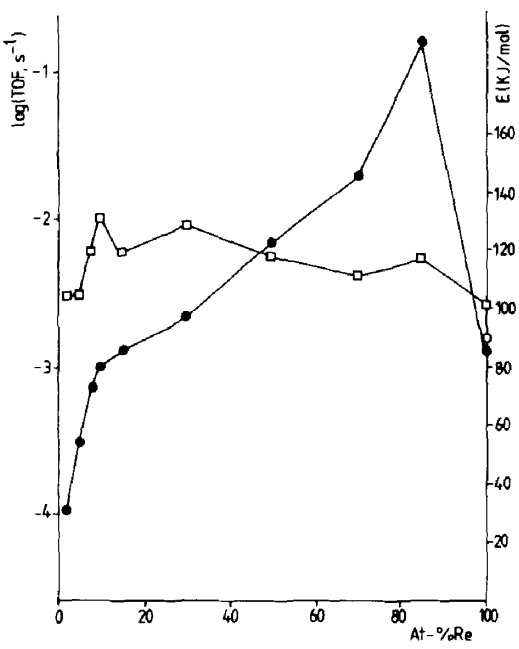

FIG. 9. The energy of activation (□) and TOF (●) in the CO + H_2 reaction vs composition measured at 540 K on CaO-containing samples. (○) TOF for Ca-free Re sample.

ethane is steeper than that for cyclohexane dehydrogenation.

After heat treatment at 920 K, the calcium-containing samples become completely inactive. One of the reasons is a large decrease in the surface area compared to the samples prepared by the standard method (see Fig. 6). The second explanation is the Ca enrichment on the surface which covers the metallic sites measured by XPS.

It has to be noted that the TOF for dehydrogenation, hydrogenation, and for hydrogenolysis on 85 at.% Re samples is the same or higher than on the calcium-free samples (*17*), but this correlation is reversed when the nickel concentration is above 50 at.%. An increase in the amount of nickel results in a rise in the overall CaO concentration which is further enhanced by surface segregation leading eventually to a serious activity loss on the Ni-rich samples. However, in the range between 0 and 50 at.% Re the TOF of ethane hydrogenolysis is significantly lower than those calculated for the other hydrocarbon reactions, i.e., hydrogenolysis in this range is suppressed.

In the CO + H_2 reaction the catalysts first have to be stabilized because after the admission of the reaction mixture serious deactivation occurs mainly on pure Ni and on Ni-rich samples. In Fig. 9 the TOF values measured at 540 K are plotted vs composition. Practically no difference between 100 at.% Re and the Re + Ca samples can be observed. Reliable rate data for rhenium-free nickel are not available due to the continuous deactivation. From the composition of 2 at.% Re the TOF sharply increases and there is a small but not significant fluctuation in the apparent energy of activation (see Fig. 9).

Selectivity data on the CO + H_2 reaction give additional information about the effect of rhenium. By decreasing the nickel concentration to 85 at.% Ni the increase in the TOF is accompanied by a preferred chain formation indicated by the slight increase in $S_{C_2^+}$ (see Fig. 10). Further decrease of nickel causes an increase in methane selectivity ($1 - S_{C_2^+}$). By considering the olefin selectivity it is clearly seen that higher hydrocarbons consist mainly of saturated molecules. Although nickel is considered as a methanation catalyst, higher hydrocarbons are also produced here which might be ascribed to the presence of calcium.

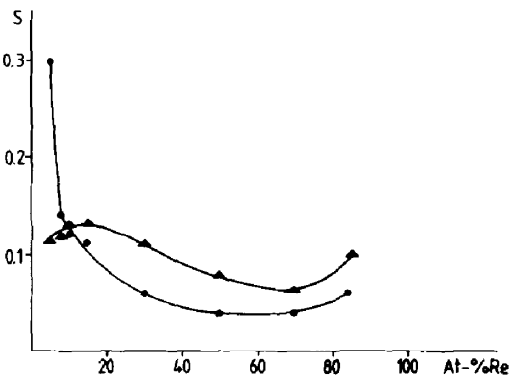

FIG. 10. Selectivity changes in the CO + H_2 reaction vs composition on the Ca-containing samples measured at 540 K. Symbols: (▲) $S_{C_2^+}$ and (●) $S_{olef.}$.

DISCUSSION

In the nickel–rhenium bimetallic system both enhanced dispersion and alloy formation were observed as the amount of rhenium added to nickel increased (*1–3*). As calcium oxide is introduced to the bimetallic samples, the dispersion is further increased as indicated by the crystallite size measured by X-ray line-broadening, by BET surface area and by the CO chemisorption data representing the metal sites exposed at the surface.

Stabilization of the higher dispersion starts already in the first step of catalyst preparation. On addition of calcium to nickel carbonate before decomposition in air at 770 K the sintering of NiO is prevented most probably via the formation of a mixed surface oxide phase. A similar effect has been found by McVicker *et al.* (*19*) for iridium catalysts when the sintering of iridium during oxidative treatment was prevented by trapping IrO_2 in the form of calcium iridate. On subsequent reduction of the CaO + NiO mixture the sintering of the nickel particles formed is hindered as CaO covers the surface. CaO also prevents complete reduction of the mixed oxide phase as XPS shows about 5–10% of the nickel to be in an oxidized state.

In addition to the increase of dispersion, alloy formation between Ni and Re is also favored by CaO. The increase in the lattice distance and the decrease in magnetization shown in Figs. 1 and 2, respectively, are strong evidence for this effect which is further supported by the B.E. shift found in XPS. In the literature a shift in the core level binding energies has been described for other systems (*20*).

In the interpretation of the catalytic results two effects have to be taken into consideration for calcium-free bimetallic samples: (i) increased dispersion caused by the addition of a small amount of rhenium to nickel, and (ii) on rhenium-rich samples alloy formation between nickel and rhenium. These effects are reflected in the hydrocarbon reactions to different extents. In cyclohexane dehydrogenation, which is a structure-insensitive reaction (*21*), the TOF values are practically constant in the whole composition range: this is similar to other reactions involving cyclohexane such as isotope exchange on Pt (*22*), and dehydrogenation on Ni–Cu catalyst (*23*). If another effect but dispersion had been operating here, the constancy of the TOF would not have been observed. This is not the case for benzene hydrogenation, as the sharp increase in the presence of a small amount of rhenium may indicate that the intrinsic activity of the hydrogenating site increases, probably by retarding the deactivation process. In this range the effect of rhenium suggested by Bertolacini and Pellet (*24*) is likely to be operative, whereas at higher rhenium content the rhenium gradually takes over the role of active sites with low activity due to its surface enrichment. The maximum found for the hydrogenolysis of ethane is similar to what has been observed for other bimetallic rhenium-containing catalysts such as for $PtRe/Al_2O_3$ (*18*), i.e., for the sample containing 50 at.% Re the TOF for butane hydrogenolysis passes through a maximum.

Although CaO addition produces enhanced dispersion and promotes alloy formation, these effects are completely masked by the high CaO surface coverage. On the nickel-rich catalysts the hydrocarbon reactions are suppressed to a large extent. With decreasing amount of calcium oxide the metal dispersion does not change appreciably (see Fig. 7) up to 30 at.% Re. On the other hand, for the Ca-containing samples the metal surface area is always smaller than the total surface area, which is opposite to that observed for calcium-free catalysts. As it is obvious that calcium oxide covers a part of the metal sites along with the rhenium enrichment on the surface, these two effects also alter the morphology of the metallic sites, because the TOF values for the three hydrocarbon reactions are much smaller than those on the

calcium-free samples. However, the sharp decrease in the total surface area in the range between 0 and 30 at.% Re is not accompanied by a change in metal surface area. In this range, however, the TOF values are growing, which is primarily ascribed to the effect of rhenium on nickel. The increase of the TOF value cannot be attributed to the rhenium enriched on the surface, either, because the TOF drastically drops again on the pure rhenium sample.

The site blocking effect of calcium is displayed when the TOF values of hydrogenolysis and dehydrogenation are compared. The large drop of the TOF of ethane hydrogenolysis compared to that of cyclohexane dehydrogenation is due to the large decrease in the surface concentration of multiple sites responsible for hydrogenolysis.

A similar effect was also found by Margitfalvi *et al.* (*25*) if SnO_2 was present on Pt/Al_2O_3 catalysts. Credence is lent to this mechanism by the fact that after high temperature treatment, when the calcium on the surface is significantly enhanced, the catalysts become totally inactive in the hydrocarbon reactions.

Here we have to emphasize that the dehydrogenation of cyclohexane and hydrogenation of benzene, being indicative of single sites (*21*), possess higher TOF values on the catalyst of 85 at.% Re composition than those of calcium-free samples (*17*). We may therefore suggest a similar effect to that observed by van Broekhoven *et al.* (*26, 27*) and Lankhorst (*28*), i.e., a diminished self-poisoning rate is indicative of small ensembles separated by CaO on the surface.

In the $CO + H_2$ reaction the CaO-containing catalysts behave in a similar manner as in the ethane hydrogenolysis. On decreasing nickel concentration the TOF first sharply increases. There is a break point at around 10 at.% Re; then it steadily but less sharply increases up to 85 at.% Re composition. On 100 at.% Ni and 100 at.% Re (both containing CaO) the TOF is low. The catalytic activity of nickel displayed in the $CO + H_2$ reaction is stabilized by the addition of a small amount of rhenium from which we may conclude that it prevents the formation of carbonaceous deposits. Since there is a break point for the TOF at 10 at.% Re a promoter effect may be suggested at low rhenium concentration. Namely, in that range small ensembles are stabilized by the presence of CaO on the surface and thus the deactivation is less than in the range above 10 at.% rhenium concentration.

The increase of TOF for the $CO + H_2$ reaction may be attributed to two effects. As has been found for other bimetallic systems such as FeRu (*29*), CoIr (*30*), FeIr (*31*), and PtIr (*32*), the presence of the second metal prevents carbide formation, and thus deactivation processes on the bimetallic catalysts are slowed down compared to monometallic catalysts. Here, the prevention of deactivation is the main effect leading to the increase of methane formation and the decrease of olefin formation as rhenium content increases.

Second, the similarity between ethane hydrogenolysis and CO hydrogenation is not striking because both reactions are structure sensitive and the number of sites of proper size increases as CaO on the surface decreases.

In conclusion it is established that the modification of nickel–rhenium catalyst with calcium oxide results in a favored alloy formation and in an increased dispersion. Although at high nickel content there is a low activity for hydrocarbon reactions because of the high surface coverage with CaO, at lower Ni content hydrogenation and dehydrogenation are slightly promoted. However, hydrogenolysis is strongly suppressed in this range because CaO is still sufficient on the surface to separate multiple sites. For the carbon monoxide hydrogenation the TOF steadily increases, which is partly due to the reaction being structure sensitive and partly to the suppression of the deactivation process.

REFERENCES

1. Eick, J., Ph.D. thesis. Technische Hochschule "Carl Schorlemmer" Leuna-Merseburg, 1981.
2. Eick, J., and Engels, S., *Z. Anorg. Allg. Chem.* **507,** 171 (1983).
3. Eick, J., Engels, S., and Mörke, W., *Z. Anorg. Allg. Chem.* **512,** 34 (1984).
4. Nielsen, A., "Advances in Catalysis," Vol. 5, p. 1. Academic Press, New York, 1953.
5. Rostrup-Nielsen, J. R., "Steam Reforming Catalysts." Tekniks Forlag A/S, Copenhagen, 1975.
6. Guczi, L., Matusek, K., Manninger, I., Király, J., and Eszterle, M., "Preparation of Catalysts II," p. 391. Elsevier, Amsterdam, 1979.
7. Topsøe, H., Dumesic, J. A., Derouane, E. G., Clausen, B. S., Mørup, S., Villadsen, J., and Topsøe, N., "Preparation of Catalysts II," p. 365. Elsevier, Amsterdam, 1979.
8. Good, M. L., Abarnejad, M., and Donner, J. T., *Prepr. ACS Div. Pet. Chem.* **23,** 495 (1978).
9. Donner, J. T., Ph.D. thesis. Louisiana State University, 1983.
10. Bossi, A., Barbassi, F., Petrini, G., and Zanderighi, L., *in* "Proceedings, 7th International Congress on Catalysis, Tokyo, 1980," Part B, p. 1468. Kodansha/Tokyo and Elsevier/Amsterdam, 1981.
11. Basset, D. W., and Habgood, H. W., *J. Phys. Chem.* **64,** 769 (1960).
12. Savickij, E. M., Tylkina, M. A., and Povarova, K. B., "Splavy Renija," p. 136. Nauka, Moscow, 1965.
13. Scherrer, P., *Göttinger Nachrichten, Math. Phys.* **98** (1918); Spindler, H., and Bisinger, H. J., *Chem. Tech. (Leipzig)* **21,** 360 (1969).
14. Engels, S., and Mörke, W., *Phys. Status. Solidi B* **119** K109 (1983).
15. Slinkin, A. A., *Usp. Chem.* **37,** 1521 (1968).
16. Briggs, D., and Seah, M. P. "Practical Surface Analysis by Auger and X-Ray Photoelectron Spectroscopy." Wiley, Chichester, 1983.
17. Eick, J., Engels, S., and Maier, U., *Z. Chem.* **23,** 308 (1983).
18. Haining, I. H. B., Kemball, C., and Whan, D. A., *J. Chem. Res.*, 170 (1977).
19. McVicker, G. B., Garten, R. L., and Baker, R. T. K., *J. Catal.* **54,** 129 (1978).
20. Hegde, R. I., *Surf. Interface Anal.* **4,** 204 (1982).
21. Sinfelt, J. H., "Advances in Catalysis," Vol. 23, p. 91. Academic Press, New York, 1973.
22. Guczi, L., and Gudkov, B. S., *React. Kinet. Catal. Lett.* **9,** 343 (1978).
23. Sinfelt, J. H., Carter, J. L., and Yates, D. J. C., *J. Catal.* **24,** 283 (1972).
24. Bertolacini, A., and Pellet, R. J., *in* "Catalyst Deactivation" (B. Delmon and G. F. Froment, Eds.), p. 73. Elsevier, Amsterdam, 1980.
25. Margitfalvi, J., Hegedüs, M., Göbölös, S., Kern-Tálas, E., Szedlacsek, P., Szabó, S., and Nagy, F., *in* "Proceedings, 8th International Congress on Catalysis. Berlin, 1984," Vol. IV, p. 903. Verlag Chemie, Weinheim, 1984.
26. van Broekhoven, E. H., Schoonhoven, J. W. F. M., and Ponec, V., *Surf. Sci.* **156,** 899 (1985).
27. van Broekhoven, E. H., and Ponec, V., *Surf. Sci.* **162,** 731 (1985).
28. Lankhorst, P. P. de Jongste, H. C., and Ponec, V., *in* "Catalyst Deactivation" (B. Delmon and G. F. Froment, Eds.), p. 43. Elsevier, Amsterdam, 1980.
29. Guczi, L., Schay, Z., and Bogyay, I., "Preparation of Catalysts III," p. 451. Elsevier, Amsterdam, 1983.
30. Guczi, L., Matusek, K., Bogyay, I., Garin, F., Esteban-Puges, P., Girard, P., and Maire, G., *C*$_1$ *Mol. Chem.* **1,** 355 (1986).
31. Niemantsverdriet, J. W., van Kaam, J. A. C., Flipse, C. F. J., and van der Kraan, A. M., *J. Catal.* **96,** 58 (1985).
32. Engels, S., Tran-kim-Thanh, and Wilde, M., *Chem. Tech. (Leipzig)* **27,** 459 (1975).